

## Influence of Long-Range Electrostatic Treatments on the Folding of the N-Terminal H4 Histone Tail Peptide

Roberto D. Lins\* and Ursula Röthlisberger

*École Polytechnique Fédérale de Lausanne, Institute of Chemical Sciences and Engineering, CH-1015 Lausanne, Switzerland*

Received July 12, 2005

**Abstract:** A series of ca. 20-ns molecular dynamics simulation runs of the N-terminal H4 histone tail in its un- and tetraacetylated forms were performed using three different long-range electrostatic treatments namely, spherical-cutoff, reaction field, and particle mesh Ewald. Comparison of the dynamical properties of the peptide reveals that internal flexibility and sampling of the conformational space are heavily dependent on the chosen method. Among the three tested methods, the particle mesh Ewald treatment yields the least conformational variation and a structural stabilization tendency around the initially defined topological framework.

### 1. Introduction

Lattice summation methods are currently used as the standard long-range electrostatic treatment in explicit-solvent simulations using periodic boundary conditions. At least one out of a variety of implementations of the method (Ewald summation,<sup>1</sup> particle mesh Ewald (PME),<sup>2</sup> smooth particle mesh Ewald (SPME),<sup>3</sup> particle–particle particle mesh (P3M)<sup>4</sup>), originally developed for crystalline systems, has been implemented in the major biomolecular simulation softwares. Enforcing artificial periodicity by the means of lattice sum algorithms in inherent nonperiodic systems, such as explicitly solvated proteins and DNA, have been suggested to cause an unrealistic stabilization of the molecular system by reducing conformational sampling.<sup>5–9</sup> Recent studies conclude that although artificial periodicity induces a non-negligible energetic bias, it does not produce major structural perturbations in the solute.<sup>10</sup> However, the authors also state that the use of lattice sum methods overstabilize the secondary structure elements in high-temperature simulations.<sup>10</sup> In contrast, simulations of highly charged proteins<sup>11</sup> show marginal higher atomic positional fluctuations and deviations when P3M is compared to the reaction field (RF)<sup>12</sup> scheme. Most of the up-to-date conclusions are drawn based on relatively short time scale simulations (up to 3 ns) of

stable protein or DNA structures. Therefore, to access the effect of three different electrostatic treatments, spherical group charge-based cutoff without switching function (SC),<sup>13</sup> RF and PME, on the structural variation of a conformationally rich peptide, a series of ca. 20 ns long explicit-solvent molecular dynamics (MD) simulations was performed. The 23-aa long amino-terminal H4 histone tail peptide was chosen for this purpose due to its small size and structural behavior change upon lysine acetylation. CD-spectra of the N-terminal H4 histone tails, in a 90% TFE (v/v) solution, show increasing helical content as a function of the number of acetylated lysines.<sup>14,15</sup> Due to its well-known  $\alpha$ -helical stabilizer properties,<sup>16–19</sup> this solvent has been widely used to examine the helical propensity of peptides. The observed 25% helical propensity for the (fully) tetraacetylated form corresponds to ca. 5–6 residues.<sup>15</sup> This number is in good agreement with the length of the consensual helical region, residues 15–21, predicted by four independent secondary structure assignment methods.<sup>15</sup> It is worth noting that, generally, short-length peptides exhibit an inherent high flexibility when immersed in high-dielectric solvents. The chosen test-case makes no exception to this rule. However, major structural features of the system have been characterized, as discussed above. While the choice of a peptide of a well-defined structure would initially seem to be the ideal choice, it might also flatten out the foreseen differences this study aims at.

The present scope lies in a systematic evaluation of the impact of different commonly used electrostatic treatments

\* Corresponding author phone: (509)375-2755; fax: (509)372-4720; e-mail: roberto.lins@pnl.gov. Present address: Pacific Northwest National Laboratory, Computational Biology and Bioinformatics, Richland, WA 99352.

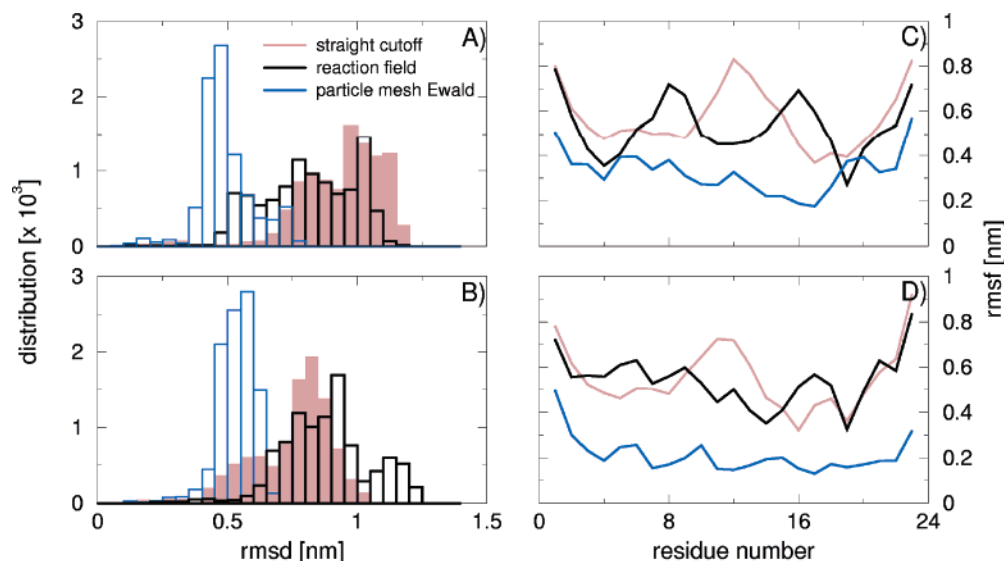


**Figure 1.** rmsd distributions for the backbone atoms of the H4 histone tail in its (A) non- and (B) tetraacetylated forms, and their corresponding rmsf (C and D, respectively), upon the three probed electrostatic treatments: SC (maroon), RF (black), and PME (blue). Analyses are displayed over the 0–18 ns window.

on conformational sampling of a biologically relevant system by the means of molecular dynamics simulations. Additionally, the results provide insights to the structure of the N-terminal H4 histone tails upon lysine acetylation.

## 2. Methods

Initial molecular dynamics simulation setups comprised the 23-residues N-terminal H4 histone tail peptide in a canonical  $\alpha$ -helical conformation in its unacetylated (*nonac*) and tetraacetylated (*ac*) forms solvated in water. (The ability of these two systems to explore the conformational space was probed using three different methodologies to treat the long-range electrostatic interactions: spherical group charge-based cutoff without switching function (SC),<sup>13</sup> reaction field (RF),<sup>12</sup> and particle mesh Ewald (PME).<sup>2</sup>) The peptides measured a maximum of 3.6 nm in their longest axis and were solvated in a  $7.0 \times 7.0 \times 7.0$  nm SPC water<sup>20</sup> box, so to provide plenty of room between its periodic images. Counterions were added to both systems in order to keep their total charge equal to zero (0  $e$ ). The unacetylated system comprised 34 064 atoms (228 protein atoms, 9  $\text{Cl}^-$  ions, and 11 275 water molecules), while the tetraacetylated system contained a total of 34 062 atoms (232 protein atoms, 5  $\text{Cl}^-$  ions, and 11 279 water molecules). The systems were energy-minimized using 200 steepest decent steps. Equilibration was performed for 5 ps each at temperature intervals of 50, 100, 150, 200, 250, and 300 K, with velocity reassignment every 0.5 ps and a 2-fs time step. Production runs ranged from 18 to 25 ns in the NpT ensemble. The temperature was maintained at 300 K by a weak coupling to two independent heat baths with relaxation times of 0.1 ps for the solvent and the solute. The pressure of the system was kept at 1 bar by isotropic coordinate scaling with a relaxation time of 0.4 ps. SHAKE constraints<sup>21</sup> with a tolerance of  $10^{-4}$  nm were applied to all bonds involving a hydrogen atom. A double twin-range cutoff of 0.8/1.4 nm was used when the long-range electrostatic interactions were treated by the cutoff-based methods (SC and RF). The short-range neighbor-list

was updated every step, and the long-range one every 5 steps. A 1.0 nm cutoff was used as a short-range cutoff when PME was employed in the treatment of the long-range electrostatic contributions. All simulations were carried out using the GROMOS96 43A1 force field<sup>22</sup> within the Gromacs 3.2.1 package.<sup>23</sup> Coordinate frames were saved every 0.2 ps for analysis. The secondary structure content maps shown in the paper were performed via the DSSP program<sup>24</sup> implemented in the Gromacs program, version 3.2.1.<sup>23</sup>

## 3. Results and Discussion

The amount of conformational sampling was accessed via the root-mean-square deviation (rmsd) distribution for the backbone atoms over the 0–18 ns window (based on the shorter simulation) (Figure 1A,B). The PME treatment produced a narrower distribution in both the *nonac* and *ac* systems. Average rmsd is also relatively closer to its reference, i.e., a canonical  $\alpha$ -helix in this case. The corresponding root-mean square fluctuation (rmsf) (Figure 1C,D) shows a reduced flexibility of 40–60% on average for the peptide treated by PME compared to the cutoff-based methods. The average overall fluctuation in the SC simulation is only ca. 3–7% higher than in the RF one. However, individual residue flexibilities and rmsd distributions indicate that these methods sample different parts of the phase-space for a given system at the nanosecond time scale.

The behavior of the secondary structure content of the peptides was analyzed as a function of the simulation time (Figure 2). The helical content in the *nonac* system is completely abolished within 1 and 4 ns when SC (Figure 2A) and RF methods (Figure 2B) are used. The PME treatment stabilizes the helical region spanning residues 14 to 22 in a 5-helix ( $i, i+5$ ) configuration (Figure 2C). A higher helical content is observed for the acetylated form of the peptide regardless of the electrostatic treatment used. However, the actual value of helical content differs significantly. The use of SC and RF results in a  $\alpha$ -helical propensity ca. 18% (in both cases) spanning residues 14 to 19 (Figure

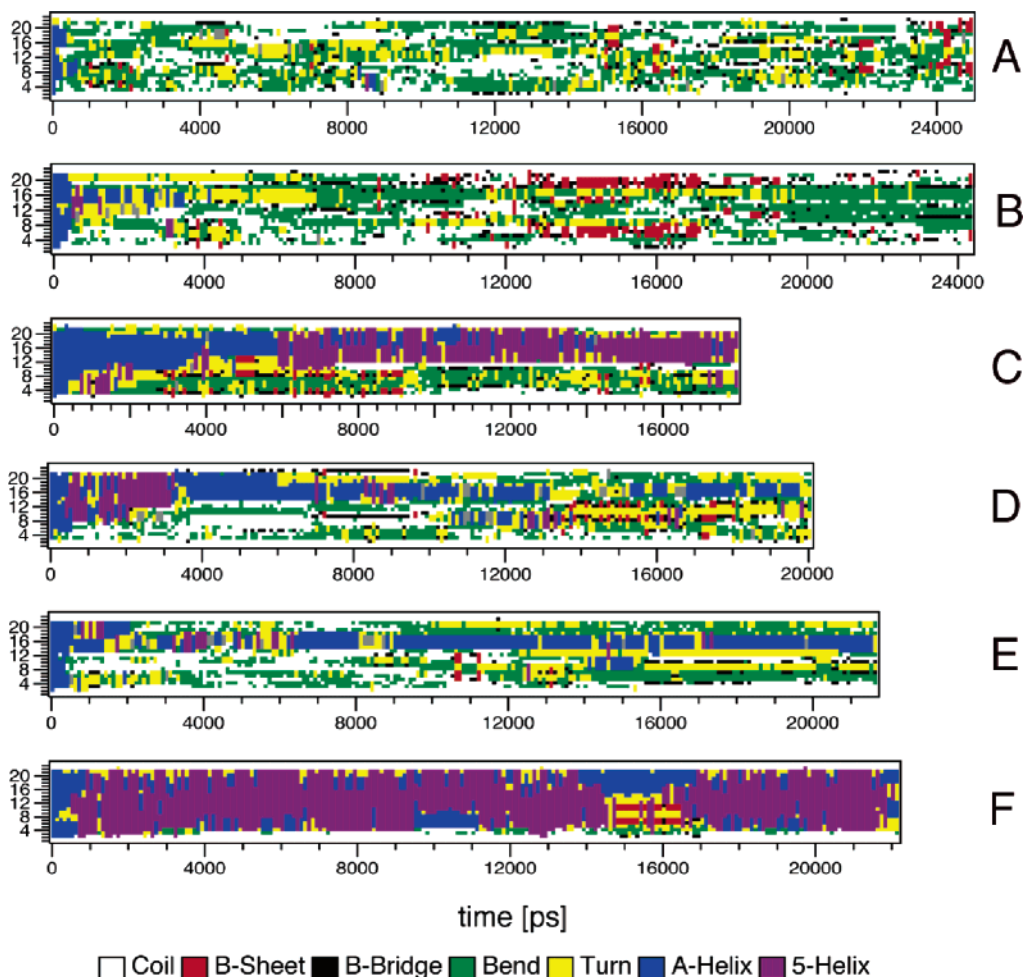


**Figure 2.** Secondary structure content for the N-terminal H4 histone tail in its unacetylated (nonac) and tetraacetylated (ac) forms as a function of the simulation time upon the three probed electrostatic treatments: (A) nonac/SC, (B) nonac/RF, (C) nonac/PME, (D) ac/SC, (E) ac/RF, and (F) ac/PME. (Secondary elements are defined according to the DSSP program.<sup>20</sup> The color-coded chart at the bottom is provided for content identification.)

2D,E). The helical occupancy is about 9% higher in the RF simulation. This increased stability may have its roots in the better energy conservation scheme used by this method over the SC one. PME treatment of the acetylated peptide is characterized by a mix of 5- and  $\alpha$ -helix structure (except for ca. 10% of the time ( $\sim 13.6$ – $17$  ns) (Figure 2F)). These findings indicate that either (i) the use of the cutoff-based methods (SC and RF, here) would produce an enhanced sampling due to energy conservation issues, or (ii) the intrinsic artifacts arisen from PME would cause a reduction in the conformational sampling. The inability to conserve energy is a well-known limitation of the SC method. However, few variations such as the RF or the more recently developed force-shifted spherical cutoff methods<sup>21</sup> have proven to keep this issue to a minimum<sup>12,25</sup> and produce conformational samplings and distributions in excellent agreement with experimental (NMR, CD, ORD, X-ray crystallography) data.<sup>25–32</sup> In addition, based on the CD-spectra and the secondary content prediction data<sup>14,15</sup> the PME treatment seems to overestimate the total helical content in these runs. It results in over 40% and 70% helical content for the nonac and ac simulations, respectively.

In a recent study, Monticelli and Colombo have compared the ability of PME- and SC-simulations of the  $\beta 3$  peptide to

reproduce experimental NOE restraints.<sup>33</sup> Based on 500-ns simulations, the use of PME allowed a better description of the experimental NOE restraints and secondary structure content than the SC simulations. A comparison of the different electrostatic methodologies was not the primary intention of this study, and no systematic assessment has been made in this direction. However, their findings suggested an overestimation of the secondary structure content, reduced flexibility, and stabilization tendency around the initial conformation when PME is used.<sup>33</sup> At the same time, the SC simulations have failed to provide an accurate description of the NOE restraints apparently due to a high flexibility.<sup>33</sup> No alternative methodology has been tested or proposed in order to overcome the problem. To evaluate this apparent overstabilization tendency from the lattice-sum method, a frame without any helical content was randomly extracted from the ac/SC simulation (at 14 280 ps) and switched to the PME treatment. A secondary structure map as a function of time of this new 23+ ns MD simulation is shown in Figure 3. The results revealed indeed an entrapment of the peptide around the newly provided topological framework.

While reverse folding is not expected in a 24+ ns MD simulation, the immutability of the completely distinct

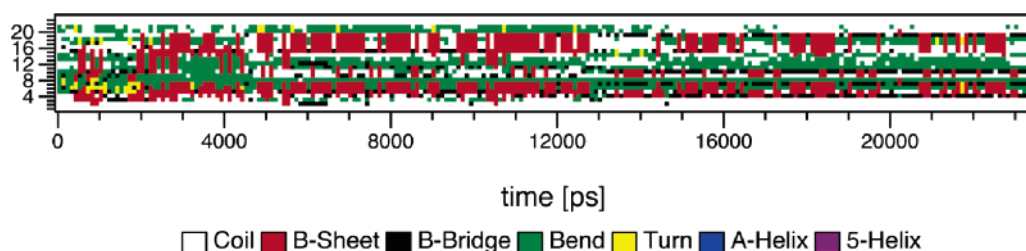


**Figure 3.** Secondary structure content for the tetraacetylated (ac) form of the N-terminal H4 histone tail as a function of the simulation time. (Secondary elements are defined according to the DSSP program.<sup>24</sup> The color-coded chart at the bottom is provided for content identification.)

secondary elements in the simulations of the same peptide displayed in Figures 2F and 3 is remarkable in such time scale, especially if compared with the cutoff-based runs shown in Figure 2.

#### 4. Conclusion

The limitations of the SC method in molecular dynamics simulations are well-established ones and known to lead to severe problems in the energy conservation scheme and unrealistic structural distortions.<sup>34–39</sup> A number of studies, using different force fields, have shown that correction methods applied outside of the cutoff sphere, such as the continuum-based reaction field and switching methods, may represent a satisfactory compromise between accuracy and the computational costs associated with the different Ewald summation methods.<sup>10,11,25,28,31</sup> This conclusion is partly due to the marginal difference observed in sampling and thermodynamical properties when comparing simulations using long-range correction techniques with PME-treated ones.<sup>10,11,28,31</sup> However, these independent studies involved either relatively short simulation times (up to 3 ns) of highly stable proteins and DNA<sup>10,11,28</sup> or enhanced sampling simulations<sup>31</sup> (high temperatures/replica-exchange algorithms). While the latter case is undeniably more efficient, it may flatten out the effect of the long-range electrostatic treatments on conformational sampling at room temperatures. Nevertheless, the exchange of replicas acceptance ratio is reported as slightly smaller for the peptides in the PME simulation in comparison to the RF ones.<sup>31</sup> It might suggest to some extent a higher overall conformational hindrance of the system treated by PME. The outcome of the simulations presented here, however, shows clearly that (i) the sampling of the conformational phase-space in a typical molecular dynamics simulation can be heavily influenced by the choice of the long-range electrostatic treatment and, consequently, (ii) that RF may not always be used as a cost-efficient alternative to PME. It is worth noting that these discrepancies in sampling are likely to be less pronounced in larger and conformationally stabler molecular systems. However, tests at the present or, ideally, longer simulation lengths would be required in order to confirm such an assumption.

In summary, the present simulations consistently show that the acetylated form of the H4 histone tail contains a higher helical content regardless of the electrostatic treatment used. This helical structure occurs toward the C-terminal region of the peptide in agreement with experimental and secondary structure prediction data.<sup>14,15</sup> The use of the SC, RF, and

PME methods, within the same time scale and at room temperature, seems to yield the exploration of different regions of the energy surface for a given system. The peptides treated by the PME scheme show the least conformational variation throughout the dynamics and a non-negligible overstabilization of the secondary structure. Sampling is reduced when compared to the SC and RF methods and, to some extent, restricted to the initial structural topology defined in the setup. Therefore, the current findings suggest that the use of cutoffs along with proper correction methods to the outside-cutoff sphere may be better suited for the sampling of the conformational space of highly flexible naturally inhomogeneous systems, such as the study of protein and peptide folding. However, substantiation of the current observation is not an easy task since it would require the similar assessment of systems that are simultaneously internally flexible and structurally well characterized. While such entities are far from abundant, in the past few years the groups of Seebach and van Gunsteren have combined NMR experiments and MD simulations to characterize the structure and dynamics of several fast-reversible-folding  $\beta$ -peptides.<sup>26,27,40,41</sup> Given the impressive level of agreement obtained between theory and experimental data, even when looking at different temperatures, it places these non-natural peptides as a potential test-case system for this type of study. Being currently limited to the nano/microsecond time scale the understanding of the influence of different electrostatic methods on the dynamics of biomolecules becomes imperative. The problem deepens if the effect of temperature and/or pressure is added, which is the case in multiple-replica MD simulations. Efforts are currently being made in this direction and shall be reported soon.

**Acknowledgment.** R.D.L. would like to thank Dr. Thereza Soares, Dr. Philippe Hünenberger, and Dr. Maurício Coutinho-Neto for insightful discussions.

#### References

- (1) Ewald, P. P. *Ann. Phys.* **1921**, 64, 253–287.
- (2) Darden, T. A.; York, D.; Pedersen, L. G. *J. Chem. Phys.* **1993**, 98, 10089–10092.
- (3) Essman, U.; Perera, L.; Berkowitz, M. L.; Darden, T. A.; Lee, H.; Pedersen, L. G. *J. Chem. Phys.* **1995**, 103, 8577–8593.
- (4) Hockney, R. W.; Eastwood, J. W. *Computer simulation using particles*; McGraw-Hill: New York, 1981.
- (5) Brooks, C. L. *Curr. Opin. Struct. Biol.* **1995**, 5, 211–215.



- (6) LouiseMay, S.; Auffinger, P.; Westhof E. *Curr. Opin. Struct. Biol.* **1996**, *6*, 289–298.
- (7) Auffinger, P.; LouiseMay, S.; Westhof, E. *J. Am. Chem. Soc.* **1996**, *118*, 1181–1189.
- (8) De Bakker, P. I. W.; H  nenberger, P. H.; McCammon, J. A. *J. Mol. Biol.* **1999**, *285*, 1811–1830.
- (9) H  nenberger, P. H.; McCammon, J. A. *Biophys. Chem.* **1999**, *78*, 69–88.
- (10) Kastenholz, M. A.; H  neneberger, P. H. *J. Phys. Chem. B* **2004**, *108*, 774–788.
- (11) Gargallo R.; H  nenberger P. H.; Aviles, F. X.; Oliva B. *Protein Sci.* **2003**, *12*, 2161–2172.
- (12) Tironi I. G.; Sperb R.; Smith P. E.; van Gunsteren W. F. *J. Chem. Phys.* **1995**, *102*, 5451–5459.
- (13) Allen M. P.; Tildesley D. J. *Computer Simulation of Liquids*; Clarendon Press: Oxford, 1987.
- (14) Cary, P. D.; Crane-Robinson, C.; Bradbury, E. M.; Dixon, G. H. *Eur. J. Biochem.* **1982**, *127*, 137–143.
- (15) Wang, X.; Moore, S.; Laszczak, M.; Ausi  , J. *J. Biol. Chem.* **2000**, *275*, 35013–35020.
- (16) Nelson, J. W.; Kallenbach, N. R. *Biochemistry* **1989**, *28*, 5256–5261.
- (17) Lehrman, S. R.; Tuls, J. L.; Lund, M. *Biochemistry* **1990**, *29*, 5590–5596.
- (18) Segawa, S.; Fukuno, T.; Fujiwara, K.; Noda, Y. *Biopolymers* **1991**, *31*, 497–509.
- (19) Sonnichsen, F. D.; van Eyk, J. E.; Hodges, R. S.; Skyes, B. D. *Biochemistry* **1992**, *31*, 8790–8798.
- (20) Berendsen, H. J. C.; Potsma, J. P. M.; van Gunsteren, W. F.; Hermans, J. In *Intermolecular Forces*; Pullman, B., Ed.; Reidel: Dordrecht, p 331.
- (21) Ryckaert, J. P.; Ciccotti, G.; Berendsen, H. J. C. *J. Comput. Phys.* **1977**, *23*, 327–341.
- (22) Daura, X.; Mark, A. E.; van Gunsteren, W. F. *J. Comput. Chem.* **1998**, *19*, 535–547.
- (23) Lindahl, E.; Hess, B.; van der Spoel, D. *J. Mol. Mod.* **2001**, *7*, 306–317.
- (24) Kabsh, W.; Sander, C. *Biopolymers* **1983**, *22*, 2577–2637.
- (25) Beck, D. A.; Armen R. S.; Daggett V. *Biochemistry* **2005**, *44*, 609–616.
- (26) Daura, X.; Gademann, K.; Jaun, B.; Seebach, D.; van Gunsteren, W. F. *Angew. Chem. Int. Ed.* **1999**, *38*, 238–240.
- (27) Daura, X.; van Gunsteren, W. F.; Mark, A. E. *Proteins* **1999**, *15*, 269–280.
- (28) Walser, R.; H  nenberger, P. H.; van Gunsteren, W. F. *Proteins* **2001**, *44*, 509–519.
- (29) Chandrasekar, I.; Kastenholz, M.; Lins, R. D.; Oostenbrink, C.; Schuler, L. D.; Tieleman, P. D.; van Gunsteren, W. F. *Eur. Biophys. J.* **2003**, *32*, 67–77.
- (30) Soares, T. A.; H  nenberger, P. H.; Kastenholz, M.; Krautler, V.; Lenz, T.; Lins, R. D.; Oostenbrink, C.; van Gunsteren, W. F. *J. Comput. Chem.* **2005**, *26*, 725–737.
- (31) Baumketner, A.; Shea, J.-E. *J. Phys. Chem. B* **2005**, *109*, 21322–21328.
- (32) Lins R. D.; H  nenberger P. H. *J. Comput. Chem.* **2005**, *26*, 1400–1412.
- (33) Monticelli, L.; Colombo, G. *Theor. Chem. Acc.* **2004**, *112*, 145–157.
- (34) Loncharich, R. J.; Brooks, B. R. *Proteins* **1989**, *6*, 32–45.
- (35) Cheetham, T. E., III.; Brooks, B. R. *Theor. Chem. Acc.* **1998**, *99*, 279–288.
- (36) Smith, P. E.; Pettitt, B. M. *J. Chem. Phys.* **1991**, *95*, 8430–8441.
- (37) Schreiber, H.; Steinhauser, O. *Biochemistry* **1992**, *31*, 5856–5860.
- (38) York D. M.; Wlodawer A.; Pedersen L. G.; Darden T. A. *Proc. Natl. Acad. Sci. U.S.A.* **1994**, *91*, 8715–8718.
- (39) Cheetham, T. E., III.; Miller, J. L.; Fox, T.; Darden, T. A.; Kollman, P. A. *J. Am. Chem. Soc.* **1995**, *117*, 4193–4194.
- (40) Daura, X.; Jaun, B.; Seebach, D.; van Gunsteren W. F.; Mark, A. E. *J. Mol. Biol.* **1998**, *280*, 925–932.
- (41) Daura, X.; Gademan, K.; Schaefer, H.; Jaun, B.; Seebach, D.; van Gunsteren W. F. *J. Am. Chem. Soc.* **2001**, *123*, 2393–2404.

CT0501699